Anal. Chem. **2008,** *80,* 2452−2456

Chemical Separations by Bubble-Assisted Interphase Mass-Transfer

David A. Boyd,*,† James R. Adleman,† David G. Goodwin,† and Demetri Psaltis†,‡

Division of Engineering and Applied Science, California Institute of Technology, Pasadena, California 91125, and School of Engineering, Ecole Polytechnique Fédérale de Lausanne, Lausanne, Switzerland

We show that when a small amount of heat is added close to a liquid−vapor interface of a captive gas bubble in a microchannel, interphase mass-transfer through the bubble can occur in a controlled manner with only a slight change in the temperature of the fluid. We demonstrate that this method, which we refer to as bubble-assisted interphase mass-transfer (BAIM), can be applied to interphase chemical separations, e.g., simple distillation, without the need for high temperatures, vacuum, or active cooling. Although any source of localized heating could be used, we illustrate BAIM with an all-optical technique that makes use of the plasmon resonance in an array of nanoscale metal structures that are incorporated into the channel to produce localized heating of the fluid when illuminated by a stationary low-power laser.

Chemical separations involving phase changes are widely used in a multitude of chemical, biological, and material syntheses. In distillation, for example, the vapor phase can be achieved by heating the liquid or, in the case of temperature-sensitive systems, by placing the liquid under vacuum. However, either method of volatilization may not be acceptable in systems that are both temperature sensitive and require the presence of dissolved gases. Furthermore, efficient collection of the vapor requires active cooling to inhibit evaporation of volatile components from small droplets.[1]

Here we report a method for achieving interphase mass-transfer at both ambient temperature and pressure and without the need for active cooling for complete recovery of the vapor. Interphase mass transport within a liquid enclosure can occur as fluid from a warmer portion of the interface is vaporized and then condensed on a cooler portion.[2] Such mass flows in nucleated vapor bubbles have been used to describe the enhanced heat transfer from a heated solid surface to a liquid during boiling.[3] Clearly, the high temperatures required to form and maintain a vapor bubble are prohibitive for temperature-sensitive systems. However, in principle, the mass-transfer is not limited to a vapor bubble but can be applied to an ambient temperature gas bubble as well.

Using a microfluidic approach, we demonstrate that a gas bubble can support interphase mass-transfer with only a slight temperature imbalance within the bubble. Unlike a vapor bubble, a gas bubble bounded by the walls of a microfluidic channel can provide stable liquid−vapor interfaces without the need for heat input to form and maintain the phase separation. At equilibrium, there is no net mass-transfer between the liquid and vapor phases. However, as we will show, by adding only a small heat flux near a liquid−vapor interface, mass transport can occur in the same manner as with a vapor bubble. Keeping the distance between the opposite liquid−vapor interfaces of the bubble small allows the vapor to be completely recondensed on the opposite interface and converted into a continuous flow of fluid along the channel. The method provides a simple means for efficient separations with minimal heating of the fluid and without the need for vacuum and active cooling for recovery of the vapor. We refer to this process as bubble-assisted interphase mass-transfer (BAIM).

We show that it is sufficient to apply heat only near the liquid−vapor interface of the bubble to drive the BAIM process. Evaporation, unlike boiling, is a surface phenomena, and microfluidics is naturally suited for accessing the liquid in the immediate vicinity of a liquid−vapor interface, and adding energy in this region allows some of it to go directly into the latent heat of vaporization. We present a system where heating is provided by a stationary, low-power laser. The conversion medium for the photothermal heating used in these studies is an array of metal nanoparticles on the surface of a microfluidic chip. The BAIM process is not exclusive to photothermal heating, and any source of localized heating will suffice.

EXPERIMENTAL SECTION

A schematic of the microchannel system is illustrated in Figure 1. The system consists of a microfluidic channel, which has a quasi-ordered array of gold nanoparticles that are incorporated into the base, and a captive gas bubble. A laser with a frequency near the plasmon resonant frequency of the nanoparticles array is focused near the edge of a gas bubble, either through the channel or the base, on the particles, causing them to be heated. The heat from the nanoparticles is transferred to the surrounding fluid causing evaporation from the surface near the laser and subsequent condensation on the far surface of the bubble. (We note that the convention for all the images in this paper of having the fluid supply on the left side of the air bubble.)

The channels were cast in poly(dimethylsiloxane) (PDMS) and sealed to a glass substrate coated with an array of Au nanopar-

* To whom correspondence should be addressed. E-mail: daboyd@caltech.edu.
† California Institute of Technology.
‡ School of Engineering, Ecole Polytechnique Fédérale de Lausanne, Lausanne, Switzerland.

(1) Wootton, R. C. R.; deMello, A. J. *Chem. Commun.* **2004**, 266−267.
(2) Plsesset, M. S.; Prosperetti, A. *J. Fluid Mech.* **1976**, *78*, 433−444.
(3) Bankoff, S. G. *AIChE J.* **1962**, *8*, 63−65.

10.1021/ac702174t CCC: $40.75
Published on Web 03/06/2008

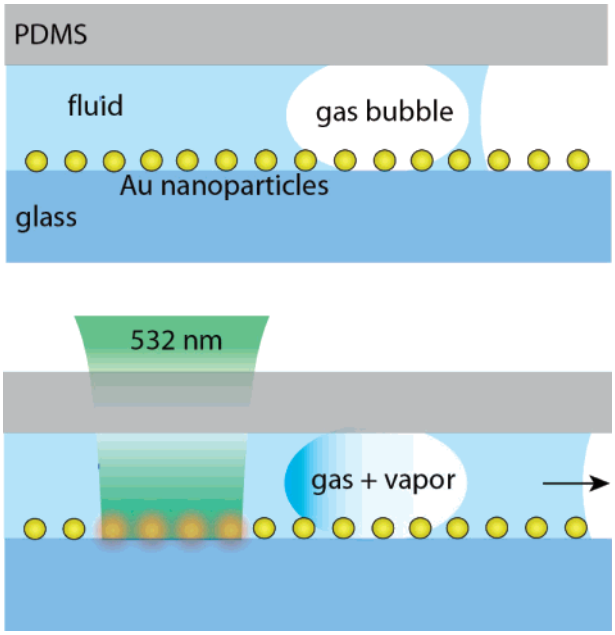

Figure 1. Schematic of the microchannel assembly (side view). An array of nanoparticles is placed on a glass slide, which serves as the base of the channel (top). A laser near the resonant frequency of the nanoparticle array is focused on the substrate, heating the particles. The heat from the nanoparticles is transferred to the surrounding fluid resulting in evaporation into the gas bubble. The vapor is subsequently condensed on the opposite side of the bubble causing an increase in the volume of the fluid to the right of the bubble and a corresponding movement to the right of the position of the free surface of the fluid column, the far right interface.

ticles, which was created by block copolymer lithography.[4] The average particle diameter was 14.5 nm with an average spacing of 46 nm. (A plot of the nanoparticle size distribution can be found in the Supporting Information (SI)). The width of the channels in these experiments was 30 μm, and the height was 5 μm. Unless noted otherwise, deionized water was used exclusively as the working fluid. A 532 nm laser which is close to the plasmon resonant frequency of the gold nanoparticle arrays, was focused through the glass substrate onto the gold nanoparticle layer. The power at the sample was 14 mW, and the diameter of the beam spot was $\sim$ 10 μm. (Details of the fabrication and experiment can be found in the SI)

Air bubbles were formed in the liquid by trapping air in the partially filled channel. To do so, we placed the laser spot near the free surface of the liquid, causing evaporation and recondensation on the channel walls 10−30 μm away. The droplets grew together to form a continuous liquid plug, trapping an air bubble with a width of 10−20 μm between the original free surface and the plug. This process is illustrated in Figure 2. It should be noted that the mass-transfer process we have described does not require gas bubbles to be formed in this manner, and in principle, gas bubbles could be injected into the channel.

RESULTS AND DISCUSSION

Placing the laser several micrometers behind the captive air bubble allowed steady mass-transfer across the bubble, increasing

(4) Jaramillo, T. F.; Baeck, S.-H.; Cuenya, B. R.; McFarland, E. W. *J. Am. Chem. Soc.* **2003**, *125*, 7148−7149.

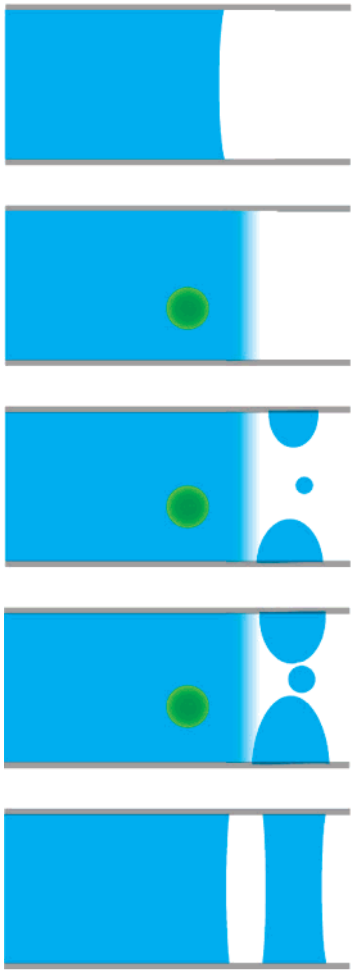

Figure 2. Schematic of the process for forming a captive air bubble used in this experiment (view from above). Starting with a still channel (top), the laser is placed near the free surface of the liquid. Local laser heating of the nanoparticles causes accelerated evaporation of the free surface (light blue), and vapor recondenses on the channel walls 10−30 μm from the surface. The droplets on the walls tend to grow together into a continuous liquid slug, trapping an air bubble with a size of $\sim$10−20 μm (bottom).

the volume of fluid on the opposite side. This process is illustrated in Figure 3. This "pumping" action can be continued indefinitely, as liquid from the supply reservoir will replace the vapor that passes through the bubble. We did not observe the pump stall even when the column of pumped fluid was several millimeters in length. The maximum volume of fluid pumped in these experiments was a few nanoliters and was limited by the length of the channels, which was $\sim$10 mm. It should be noted that the bubble remains stationary throughout this process.

We examined the mass-transfer rate of the liquid by digitizing images of the channel using a color video camera. In particular, the position of the "free surface", i.e. the leading interface of the fluid column, which is to the far right of the bubble in Figure 1, was determined using an edge detection algorithm. Plots of the measured free-surface position against time were fit using linear regression to determine the pumping speed. For a given channel dimension, the rate of mass-transfer J can be calculated from the pumping speed. Details of the image processing techniques are found in the SI.

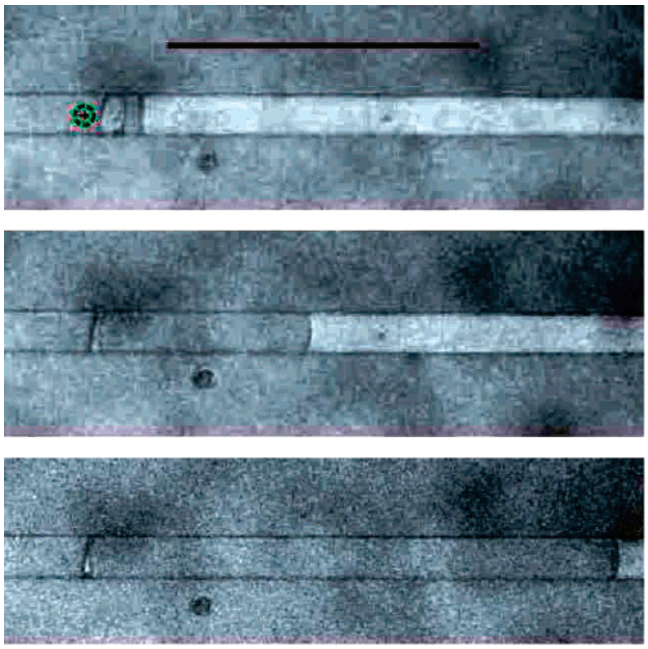

Figure 3. Images of BAIM process taken during pumping in a 40-μm channel. The scale bar, top, is 200 μm. The position of the laser spot, which is not visible, is represented as dashed outline in the top image.

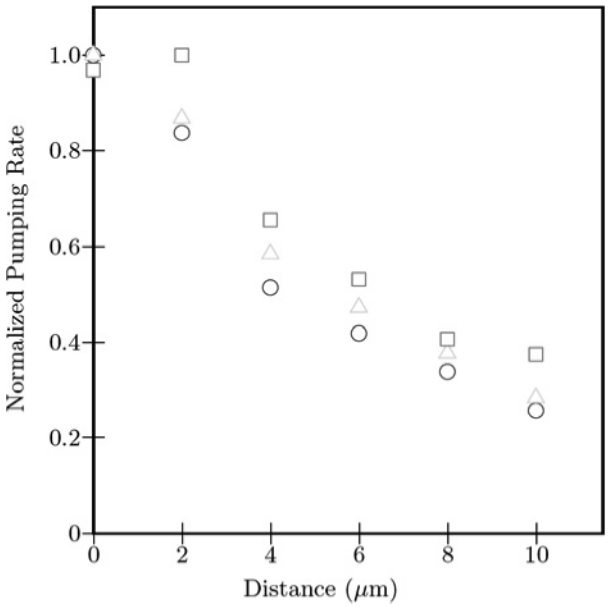

Figure 4. Dependence of the BAIM pumping rate with the position of the laser spot. During pumping, the position of the laser was moved away from the bubble by 2 μm every 10 s. The results from three separate trials are shown. Note that the absolute position of the laser spot with respect to the edge of the bubble is not necessarily the same for each trial, and the flow rate has been normalized to this position.

The measured value of J for a 30 $\times$ 5 μm channel is 4 $\times$ 10^{-4} g/(cm^2 s). Following Plesset,[5] the mass-transfer between two enclosed flat surfaces of water at different temperatures can be expressed as,

$$J = \alpha {\rho_0}^e \sqrt{\frac{RT_0}{2\pi M}} \frac{1 - (\rho_1^e/\rho_0^e)(T_1/T_0)}{1 + \sqrt{(T_1/T_0)}} \qquad (1)$$

where J (g/cm^2 s) is the mass flow rate, α is the evaporation coefficient,[6] M (kg/mol) is the molecular mass of the vapor, ρ_0^e (Pa) is the saturation vapor density at T_0 (K), the warmer interface, ρ_1^e is the saturation vapor density at T_1, the cooler interface, and R (J K^{-1} mol^{-1}) is the universal gas constant. From this equation, we see that the experimentally measured value of J is comparable to having the two surfaces of water at T_0 and T_1 = 25.0 and 25.5 °C, respectively, which assumes corresponding values of ρ_0^e and ${\rho_1}^e$ at these temperatures.

We measured the pumping rate as a function of the distance between the position of the laser spot and the edge of the bubble. During pumping, the laser was held stationary for 10 s, was translated away from the bubble by a 2 μm increment, and then this sequence was repeated. We note that the absolute position of the initial spot with respect to the edge of the bubble is not necessarily the same for each trial, and the flow rate for each trial has been normalized to the corresponding initial laser position. Beyond a distance of 10 μm from the initial position, the pumping rates were too slow to be accurately measured. The initial laser spot was kept far enough behind the liquid−air interface to avoid disturbing it. This minimal distance varied slightly for each trial, but we found that a distance of at least 5 μm was sufficient to avoid condensation of vapor inside the air bubble, which could divide the bubble into two parts.

Shown in Figure 4 is a plot of the normalized BAIM pumping rates against the relative laser position for three separate trials. The measurements show a rapid drop-off in the pumping rates as the beam is moved beyond a few micrometers from the initial spot. This result demonstrates that it is optimal to apply heat only near the interface and thereby achieving interphase mass transport without heating the entire volume of the fluid.

We observed that the bubble shrinks in the first 10 or 15 s of continuous pumping and is then stable after this initial transient. The shrinking of the bubble is presumably due to compression. We found that the flow rate is higher for smaller bubbles. In each trial in Figure 4, the bubble size does not change noticeably as we moved the laser beam away from the edge of the bubble. (We note that the bubbles are not necessarily the same size between trials, and this is in part a reason for the normalization).

If the bubbles were larger than 20 or 30 μm in width, it was observed that the evaporated liquid tended to nucleate amid the bubble, eventually dividing it into two bubbles. This could cause both bubbles to become unpinned, to be destroyed, or most often, to form two stable bubbles. We observed stable pumping in bubbles just smaller than 5 μm, but very small (2−3 μm) bubbles were often destablized and destroyed during pumping.

We examined the plasmonic heating of the fluid using temperature-sensitive fluorescence intensity measurements. A solution of ethanol and Coumarin 4 buffered with HCl and tris(hydroxymethyl)aminomethane (Tris buffer) was added to a 30 μm channel. The Coumarin 4 dye is itself pH sensitive, and the Tris buffer solution has a pH with a well-known temperature dependence. By warming the fluid, we decrease the pH, causing a decrease in

(5) Plesset, M. S. *J. Chem Phys* **1952**, *20*, 790−793.
(6) Jakubczyk, D.; Zientara, M.; Kolwas, K.; Kolwas, M. *J Atmos Sci* **2007**, *64*, 996−1004.

the intensity of the fluorescence, which we calibrated to the temperature. (See the SI for the details.) The dye was excited from below with a 405-nm laser. A band-pass filter inserted before the CCD passed only the fluorescence from the fluid and blocked both the 405 and 532 nm lasers. To prevent the evaporative effects allowed by a bubble, we examined a continuous column of fluid without a bubble, i.e., single free surface. When the beam was placed in fluid away from the free surface, we were not able to measure any significant temperature change to within 2 °C, even directly in the beam spot. When the laser beam was placed on or very close to the free surface, the free surface moved forward in the manner described by Liu et al.[7]

Excessive temperatures even of the nanoparticles themselves is a concern for bioapplications. To estimate the temperature rise of a nanoparticle by laser heating of a nanoparticle by a CW laser, we consider a model where the particle temperature is ultimately determined by the incident power density and the heat transfer from the nanoparticles to the substrate. Following the approach of Pustovalov,[8] the temperature of a spherical particle of radius r_0 due to a power density I_0 in the steady-state can be shown to be

$$T_0 = T_\infty + \frac{I_0 K_{abs} r_0}{4k_\infty} \qquad (2)$$

where K_{abs} is the efficiency absorption factor, which can be calculated from Mie scattering theory, for a particle of radius r_0 and k_∞ is the coefficient of thermal conductivity of the surrounding medium at the macroscopic equilibrium temperatureT_∞. Due to nanoscale effects that limit the heat transfer from a nanoparticle to a solid,[9,10] we can assume that most of the heat generated by the plasmon heating in the nanoparticles is transferred to the surrounding fluid. We set, $I_0 = 2 \times 10^8$ W/m^2, $r_0 = 7.5$ nm, k_∞ to be 0.61 W m^{-1} K^{-1}, and we use a value $K_{abs} = 1.5$.[11] From eq 2, the rise in the temperature of a nanoparticle $T_0 - T_\infty$ is ~1 °C. We note that these numbers are all approximate and are presented to demonstrate that results of this order are quite possible.

Using the dye solution described above, we demonstrate that BAIM offers a means for performing simple distillations. Shown in Figure 5a is a white light image of the channel, and Figure 5b is a fluorescent image of the same region before BAIM pumping of the dye solution. As the laser drove the vapor transport across the bubble, an increase in the fluorescence intensity within the liquid on the laser side of the bubble, the distilland, was measured while no fluorescence was observed on the opposite side of the bubble, the distillate, Figure 5c. Shown in Figure 5d is a plot of the change in fluorescence intensity $\Delta I/I_0$ in the distilland with time during distillation, where I_0 is the intensity at $t = 0$ s. An increase by 25% after 45 s of pumping is observed.

Although the exact composition of the distillate has not been determined, it can be clearly seen that very little if any of the dye molecule is present. Presumably the distillate contains mostly ethanol and water, which are the more volatile components of

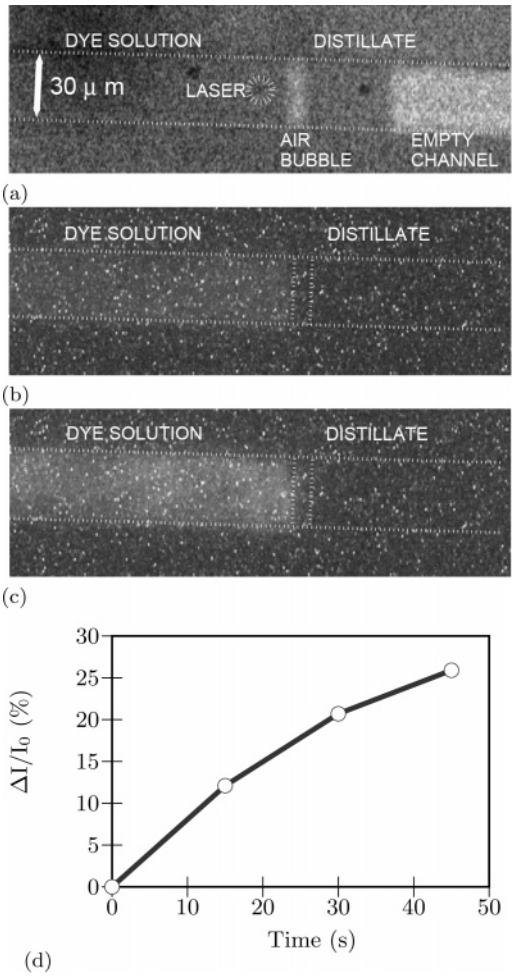

Figure 5. Example of BAIM distillation. (a) A white light image of the channel with a Coumarin dye solution. (b) The initial dye fluorescence image of this same region. (c) Fluorescence after 45 s of laser-induced evaporation. (d) The percentage increase in the mean fluorescent intensity $\Delta I/I_0$ of the distilland with time during distillation.

the dye solution. (We note that the solubility of the dye in ethanol is much greater than in water.) The presence of dye in the distillate is not expected as it has a low volatility, but more importantly, the absence of dye indicates that the integrity of the bubble is maintained during the pumping process; i.e., fluid is not able to flow along the walls of the channel. At the concentrations achieved in these experiments, neither precipitation of the dye nor a compromise in the bubble surface was observed. Since both the distilland and the distillate are recoverable, our result demonstrates that the BAIM process can be used for sample preconcentration by removal of the solvent or conversely for the purification of the solvent.

As BAIM is based on vapor transport, we believe that it is capable of separating solutions containing components of comparable volatilities, i.e., fractional distillation. Quite possibly this could be performed optimally in multiple steps with a corresponding number of bubbles spaced at least 15 μm apart operating in concert. In particular, the low-temperature nature of the BAIM distillation process makes it a possible candidate for difficult distillations, such as azeotropes. Although intrachannel distillation has been previously demonstrated, BAIM offers the advantages of (1) providing full capture of the vapor without active cooling,

(7) Liu, G. L.; Kim, J.; Lu, Y.; Lee, L. P. *Nat. Mater.* **2006**, *5*, 27−32.
(8) Pustovalov, V. K. *Chem. Phys.* **2005**, *308*, 103−108.
(9) Chen, G. *J. Heat Transfer* **1996**, *118*, 539−545.
(10) Boyd, D. A.; Greengard, L.; Brongersma, M.; El-Naggar, M. Y.; Goodwin, D. G. *Nano Lett.* **2006**, *6*, 2592−2597.
(11) Pustovalov, V. K.; Babenko, V. A. *Laser Phys. Lett.* **2004**, *1*, 516−520.

(2) requiring only a slight change in the ambient temperature of the fluid near the interface of the bubble, and (3) not requiring a carrier gas to achieve mass transport.[1]

To gain insight into the mass-transfer mechanism, it is useful to consider a few simple numerical estimates. We will assume equilibrium conditions at the vapor−liquid interface, a constant pressure inside the bubble, and a constant temperature of 25 °C. The power P required for evaporative transport is given by $P = J\Delta H$, where ΔH is the latent heat of vaporization, which for water at 25 °C is 2.4×10^6 J/kg. A flow of 5 μm/s water in a channel 30 $\times$ 5 μm corresponds to $J = 7.5 \times 10^{-13}$ kg/s. The necessary input power P is 1.8 μW. The measured absorbance A[12] of the nanoparticle arrays at 532 nm is 0.028 (See the SI for absorbance spectrum.), and we assume that the scattering from the array of particles is small and that all of the absorbed energy is converted to heat.[13] For 10 mW of input power, this gives 624 μW of power absorbed by the gold nanoparticles, indicating that there is sufficient laser energy available to account for the observed mass-transfer. We note that these estimates are presented here only to illustrate that the rates of evaporative mass-transfer of the order required to explain our results are quite likely. Clearly the pumping efficiency is low. However, this estimate does not account for temperature changes that would take place in the fluid or the significant heat transfer to the glass substrate and PDMS channel.[14]

CONCLUSIONS

We have demonstrated a new method for interphase mass transfer that can be applied to continuous flow chemical separations. The three principal advantages of the BAIM technique over existing methods are (1) that it is applicable to systems that are sensitive to temperature and vacuum, (2) that it does not require active cooling for complete recovery of the vapor phase, and (3) that heat is added to only a very small fraction of the total fluid volume. The BAIM technique makes use of microfluidics to contain a gas bubble as well as to access the liquid in the immediate vicinity of the bubble, and the simplicity and compact nature of the approach allow it to be integrated with conventional microfluidic architectures. Although, as demonstrated here, the mass-transfer rates may not be suitable for applications that require high throughput, they are, however, suitable for the study and gentle product recovery from small-scale systems, e.g., preconcentration of fragile biomolecules and bioproduct recovery from a single living cell. Much remains to be done to understand the extent of the heat losses to the fluid and support as well as determining the ability of BAIM for performing fractional distillations. These topics are the subjects of current research and will be reported at a later date.

ACKNOWLEDGMENT

This work has been generously supported by the DARPA Center for Optofluidic Integration by award HR0011-04-1-0032 and by the DARPA CAD-QT program as administered by ONR award N00014-06-1-0454. We thank Carl S. Parker for his assistance with the optical temperature measurements. We also thank George Rossman for the use of equipment and Elizabeth Miura Boyd for technical assistance.

SUPPORTING INFORMATION AVAILABLE

Additional information as noted in text. This material is available free of charge via the Internet at http://pubs.acs.org.

Received for review October 22, 2007. Accepted December 12, 2007.

AC702174T

(12) $A = \log_{10}(I_{incident}/I)$.

(13) Bohrn, C. F.; Huffman, D. R. *Absorption and scatttering of light by small particles;* Wiley: New York, 1983; pp 136−140.

(14) Erickson, D.; Stinton, D.; Li, D. *Lab Chip* **2003**, *3*, 141−149.